Measurement of Change in Wall Thickness of Cylindrical Shell Due to Cyclic Remote Actuation for Assessment of Viscoelasticity of Arterial Wall

Hideyuki Hasegawa*, Hiroshi Kanai, Yoshiro Koiwa[1] and James P. Butler[2]

Graduate School of Engineering, Tohoku University, Sendai 980-8579, Japan
[1]*Graduate School of Medicine, Tohoku University, Sendai 980-8575, Japan*
[2]*Faculty of Public Health, Harvard University, Boston, MA 02115, USA*

To characterize tissues in atherosclerotic plaques, we have developed a method, the *phased tracking method*, for measuring the strain (change in wall thickness) and elasticity of the arterial wall. However, some types of tissue, such as lipids and blood clots, cannot be discriminated from each other based only on elasticity because of the small difference in their elasticity. For more precise tissue characterization, we are attempting to measure the regional viscoelasticity. To determine viscoelastic properties, elastic moduli at multiple frequencies were obtained by generating the change in internal pressure due to remote cyclic actuation. From basic experiments using a silicone rubber tube, it was found that the change in internal pressure at the ultrasonic beam position (for measurement of the elastic modulus) can be generated by remotely applied actuation. Furthermore, from the resultant minute changes in wall thickness of less than 10 μm measured by the *phased tracking method*, elastic moduli were obtained at multiple actuation frequencies.   [DOI: 10.1143/JJAP.42.3255]

1.   Introduction

The steady increase in the number of patients with myocardial infarction or cerebral infarction, both of which are considered to be mainly caused by atherosclerosis, is becoming a serious problem. Therefore, it is important to diagnose atherosclerosis in the early stage. Computed tomography (CT) and magnetic resonance imaging (MRI) are employed for the diagnosis of atherosclerosis. Although these methods entail subjecting the patients to physical and mental hardship, they provide information only on the shape of the artery, such as the diameter of the lumen. However, the diameter of the lumen does not change by early-stage atherosclerosis.[1]

Since there are significant differences between the elastic moduli of the normal arterial wall and that affected by atherosclerosis,[2,3] evaluation of the elasticity of the arterial wall is useful in the diagnosis of early-stage atherosclerosis.[4] In addition to the diagnosis of early-stage atherosclerosis, it is also important to diagnose the vulnerability of the atherosclerotic plaque because its rupture may cause acute myocardial infarction and cerebral infarction.[5–7] The evaluation of mechanical properties, such as atherosclerotic plaque elasticity, is useful for these purposes.

To obtain the circumferential distensibility of the arterial wall in the plane perpendicular to the axial direction of the artery, measurement methods for the change in artery diameter have been proposed.[8–12] By assuming the artery to be a cylindrical shell, the average elasticity of the entire circumference in the plane has been evaluated.[13–15] However, the regional elasticity of the atherosclerotic plaque cannot be obtained by these methods because an artery with an atherosclerotic plaque cannot be assumed to be a cylindrical shell with uniform wall thickness.

To characterize tissues in the atherosclerotic plaque, a measurement method for the regional elastic modulus of the arterial wall in patients with or without an atherosclerotic plaque is needed. Such a measurement technique for the spatial distribution of the regional elasticity would be useful in the diagnosis of the vulnerability of an atherosclerotic plaque as well as for the diagnosis of early-stage atherosclerosis. For this purpose, we have developed a method, the *phased tracking method*, for measurement of the small change in arterial wall thickness (less than 100 μm) due to the heartbeat.[16–24] From basic experiments, the accuracy in measurement of the change in thickness has been found to be less than 1 μm using the *phased tracking method*.[17,20,21] From the change in thickness measured by our method, the regional strain and the elasticity of the arterial wall can be noninvasively evaluated.[23]

From the measured elastic property, it should be possible to discriminate tissues in the atherosclerotic plaque, such as fibrous tissue, lipids, and calcified tissue, from each other due to large differences in their elasticity. However, it is difficult to discriminate some tissues such as lipids and blood clots because of the small difference in their elasticity.[25] Another mechanical property of tissue which has the potential of providing useful information on discrimination of tissues is viscosity.

In the above-mentioned methods, including our method, the elastic modulus at about 1 Hz due to the heartbeat is obtained. However, it is difficult to determine viscoelastic property by measurement of the elastic modulus at only one frequency. To do so, elastic moduli at multiple frequencies should be obtained from the changes in wall thickness at multiple frequencies, which are generated by the change in internal pressure due to remote cyclic actuation.

In this study, basic experiments using a silicone rubber tube were conducted to investigate the change in internal pressure at the position where the change in wall thickness is measured using ultrasound. Such a change in internal pressure can be generated by remotely applied actuation. The resultant minute change in wall thickness was measured by the *phased tracking method*. Moreover, by sweeping the actuation frequency, the elastic moduli of the tube were measured at several actuation frequencies. Such frequency

*E-mail address: hasegawa@us.ecei.tohoku.ac.jp

characteristics of the elastic modulus have potential for the assessment of viscoelastic properties.

2. Principles

2.1 Measurement of change in wall thickness by phased tracking method

As illustrated in Fig. 1, for measurement of the small change in wall thickness, the phase shift of the echo, which is caused by displacement of an object, is estimated from two consecutive echoes.[16] For this purpose, quadrature demodulation is applied to the received ultrasonic waves reflected by the object, and then the in-phase and the quadrature signals are A/D-converted. From the demodulated signal, $z(t; d + x(t))$, reflected at a depth $d + x(t)$ at time t, where d and $x(t)$ are the initial depth set at $t = 0$ and the displacement of the object in the depth direction, the phase shift, $\Delta\theta(t)$, between two consecutive echoes is obtained from the complex cross correlation function calculated for $M + 1$ samples in the depth direction as

$$e^{j\Delta\hat{\theta}(t)} = \frac{\displaystyle\sum_{m=-M/2}^{M/2} z(t + T; d + x(t) + mD) \cdot z^*(t; d + x(t) + mD)}{\left|\displaystyle\sum_{m=-M/2}^{M/2} z(t + T; d + x(t) + mD) \cdot z^*(t; d + x(t) + mD)\right|}, \tag{2.1}$$

where D and T are the spacing of sample points in the depth direction and the pulse repetition interval, respectively, and $*$ represents the complex conjugate. In the measurement of the change in thickness, $M + 1$ in eq. (2.1) is set at 5 ($= 0.4\,\mu s$) in consideration of the pulse length of $0.46\,\mu s$.

From the estimated phase shift, $\Delta\hat{\theta}(t)$, the velocity, $v(t)$, of the object is obtained as

$$\hat{v}(t) = -\frac{c_0}{2\omega_0}\frac{\Delta\hat{\theta}(t)}{T}, \tag{2.2}$$

where ω_0 and c_0 are the center angular frequency of the ultrasonic pulse and the speed of sound, respectively.

In the estimation of the phase shift using eq. (2.1), the object position is tracked by the integration of the average velocity, $v(t)$, during the pulse repetition interval, T, as

$$\begin{aligned}\hat{x}(t + T) &= \hat{x}(t) + \hat{v}(t) \times T \\ &= \hat{x}(t) - \frac{c_0}{2\omega_0}\Delta\hat{\theta}(t).\end{aligned} \tag{2.3}$$

From the displacements, $x_A(t)$ and $x_B(t)$, of two points, which are set in the arterial wall along an ultrasonic beam, the small change in thickness, $\Delta h(t)$, between these two points is obtained as

$$\begin{aligned}\Delta\hat{h}(t) &= \hat{x}_A(t) - \hat{x}_B(t) \\ &= \int_0^t \{\hat{v}_A(t) - \hat{v}_B(t)\}\mathrm{d}t.\end{aligned} \tag{2.4}$$

2.2 Elastic modulus obtained by measured change in wall thickness

From the measured change in wall thickness, the circumferential elastic modulus is obtained as follows:[23] Under *in vivo* conditions, the artery is strongly restricted in the axial direction. Therefore, a two-dimensional stress-strain relationship can be assumed.

Under such conditions, the radial incremental strain, $\Delta\varepsilon_r(t)$, which is defined by dividing the change in thickness, $\Delta h(t)$, by the thickness of the wall, h_0, at the end diastole, is expressed by the radial and circumferential incremental stresses, $\Delta\sigma_r(t)$ and $\Delta\sigma_\theta(t)$, as

$$\begin{aligned}\Delta\varepsilon_r(t) &= \frac{\Delta h(t)}{h_0} \\ &= \frac{\Delta\sigma_r(t)}{E_r} - \nu\frac{\Delta\sigma_\theta(t)}{E_\theta},\end{aligned} \tag{2.5}$$

where E_r, E_θ, and ν are the radial and circumferential elastic moduli and Poisson's ratio, respectively.

From the change in internal pressure, $\Delta p(t)$, the circumferential and the radial incremental stresses, $\Delta\sigma_r(t)$ and $\Delta\sigma_\theta(t)$, are expressed as

$$\Delta\sigma_\theta(t) = \frac{r_0}{h_0}\Delta p(t), \tag{2.6}$$

$$\Delta\sigma_r(t) = -\frac{1}{2}\Delta p(t). \tag{2.7}$$

By substituting eqs. (2.6) and (2.7) into eq. (2.5), eq. (2.5) is rewritten as

$$\Delta\varepsilon_r(t) = -\frac{1}{2}\frac{\Delta p(t)}{E_r} - \nu\frac{r_0}{h_0}\frac{\Delta p(t)}{E_\theta}. \tag{2.8}$$

By assuming that the arterial wall is incompressible ($\nu \approx 0.5$) and elastically isotropic ($E_r \approx E_\theta$), the elastic modulus, E_θ^h, obtained from the change in wall thickness is defined as
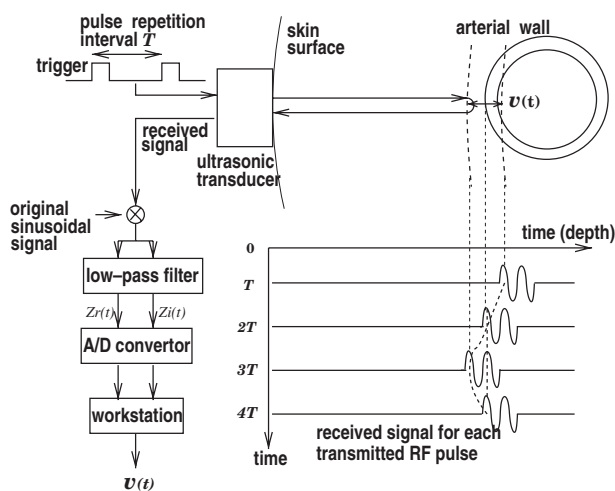

Fig. 1. Schematic diagram of the *phased tracking method*.

$$E_\theta^h = \left(\nu \frac{r_0}{h_0} + \frac{1}{2} \frac{E_r}{E_\theta} \right) \frac{\Delta p(t)}{-\Delta \varepsilon_r(t)}$$

$$\approx \frac{1}{2} \left(\frac{r_0}{h_0} + 1 \right) \frac{\Delta p(t)}{-\dfrac{\Delta h(t)}{h_0}}, \qquad (2.9)$$

where r_0 is the inner radius at the end diastole.

When we describe the changes in wall thickness, $\Delta h(t)$, and internal pressure, $\Delta p(t)$, as complex sinusoidal functions, $\Delta h_0 \cdot e^{j(2\pi f_{ac} t - \theta)}$ and $\Delta p_0 \cdot e^{j2\pi f_{ac} t}$, at an actuation frequency, f_{ac}, eq. (2.9) can be rewritten as the complex elastic modulus as

$$E_\theta^h = \frac{1}{2} \left(\frac{r_0}{h_0} + 1 \right) \frac{\Delta p_0}{\dfrac{\Delta h_0}{h_0}} \cdot e^{j\theta}, \qquad (2.10)$$

where Δh_0 and Δp_0 are the amplitude of the change in wall thickness and that of the change in internal pressure, respectively, and θ is the phase difference between changes in internal pressure, $\Delta p(t)$, and wall thickness, $\Delta h(t)$.

In this paper, the absolute value, $|E_\theta^h|$, of the complex elastic modulus defined by eq. (2.10) is obtained from Δh_0 and Δp_0, which are measured at each actuation frequency, f_{ac}.

3. Experimental Setup

3.1 Experimental system for basic experiments

The experimental system for basic experiments using a silicone rubber tube is illustrated in Fig. 2. In this system, the change in pressure inside the silicone rubber tube is generated by compressing a rubber balloon, which is placed
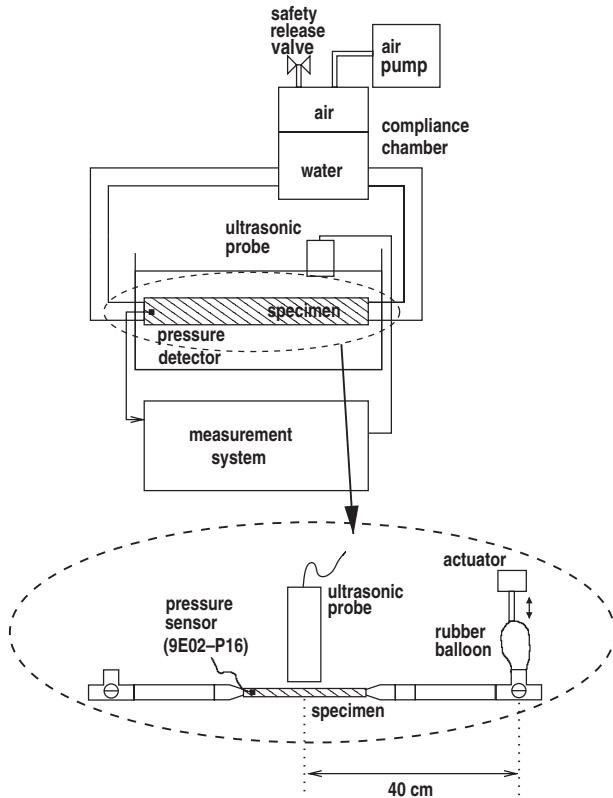

Fig. 2. Experimental system for basic experiments.

40 cm away from the ultrasonic probe, with an actuator. This system simulates measurement of the change in wall thickness of the carotid artery due to the remote actuation applied at the brachial artery. The change in wall thickness due to the resulting change in internal pressure is measured using ultrasound, and the internal pressure is also measured using a pressure transducer (NEC 9E02-P16) placed inside the tube. From the measured changes in wall thickness and internal pressure, elastic modulus can be obtained using eq. (2.10).

3.2 Measurement system

An ultrasonic pulse (center frequency: 7.5 MHz) was transmitted and received by the ultrasonic probe of standard ultrasonic diagnostic equipment (TOSHIBA SSH-140A). The received signal was amplified and demodulated. The resultant in-phase and quadrature signals were simultaneously A/D-converted with a 12-bit A/D converter at a sampling frequency of 10 MHz. The measured digital signals were inputted into a computer, and the change in wall thickness was obtained by applying the *phased tracking method*, described in §2.1, to these digital signals.

3.3 Experimental system for pressure diameter test

In order to validate the elastic modulus, $|E_\theta^h|$, measured by the *phased tracking method*, the elastic modulus of the tube was also evaluated by testing the relationship between internal pressure and external diameter. The measurement system is illustrated in Fig. 3. In this experiment, the relationship between internal pressure and external diameter was tested by generating the change in the internal pressure by compressing a rubber balloon using an actuator. The internal pressure and the external diameter were measured using a pressure transducer (NEC 9E02-P16) and a laser line gauge (KEYENCE VG-035). From the obtained relationship, the elastic modulus in the circumferential direction was evaluated based on the incremental elastic modulus, E_{inc}, defined as[13,26]

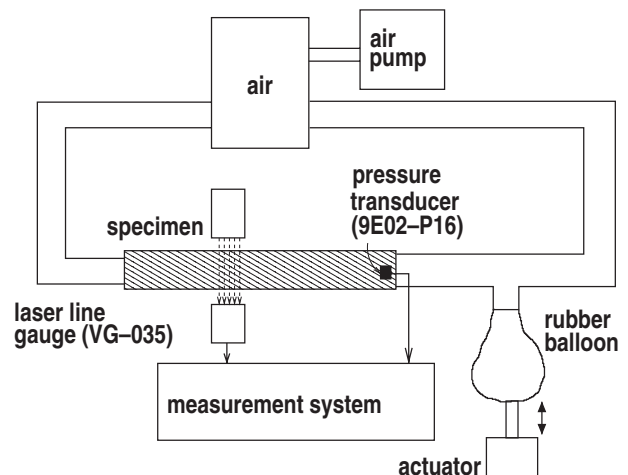$$E_{inc} = \frac{3}{2} \frac{r_0^2 r_e}{r_e^2 - r_0^2} \frac{\Delta p(t)}{\Delta r_e(t)}, \qquad (3.1)$$

Fig. 3. Experimental system employed for testing the relationship between internal pressure, $\Delta p(t)$, and external diameter, $2\Delta r_e(t)$.

where r_e and r_0 are the external and inner radii at the end diastole, respectively, and $\Delta r_e(t)$ is the change in external radius from r_e.

As in eq. (2.10), eq. (3.1) is rewritten by describing $\Delta r_e(t) = \Delta r_{e0} \cdot e^{j(2\pi f_{ac}t - \theta)}$ and $\Delta p(t) = \Delta p_0 \cdot e^{j2\pi f_{ac}t}$ as

$$E_{inc} = \frac{3}{2} \frac{r_0^2 r_e}{r_e^2 - r_0^2} \frac{\Delta p_0}{\Delta r_{e0}} \cdot e^{j\theta}, \tag{3.2}$$

where Δr_{e0} is the amplitude of the change in external diameter.

4. Basic Experiments Using a Silicone Rubber Tube

Figure 4 shows the B-mode image of a silicone rubber tube. By setting the ultrasonic beam position as shown in Fig. 4, the M-mode image was obtained as shown in Fig. 5(a). Figure 5(b) shows the measured internal pressure. From Fig. 5(b), it is found that the change in internal pressure at the measurement position can be generated by remotely applied actuation. By setting two points, A and B, along the ultrasonic beam at $t = 0$ in the M-mode image, the
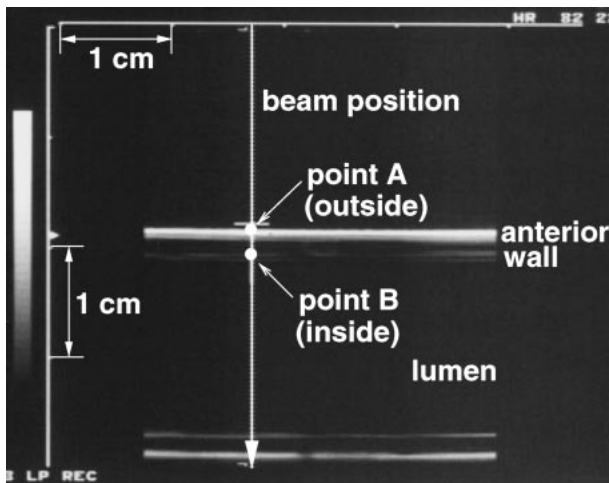

Fig. 4.   B-mode image of the silicone rubber tube.

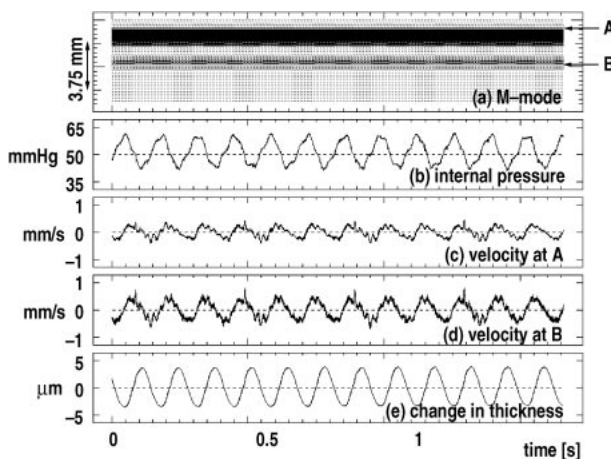

Fig. 5.   (a) M-mode image of the silicone rubber tube. (b) Internal pressure. (c) Velocity, $v_A(t)$, of point A. (d) Velocity, $v_B(t)$, of point B. (e) Change in thickness, $\Delta h(t)$, of the anterior wall (actuation frequency of 7.5 Hz).

velocities, $v_A(t)$ and $v_B(t)$, of these points were obtained by the *phased tracking method*, as shown in Figs. 5(c) and 5(d), respectively. The change in thickness, $\Delta h(t)$, of the anterior wall was obtained by integrating the difference between these two velocities. In Fig. 5(e), a minute change in thickness of less than 10 μm was measured at an actuation frequency of 7.5 Hz. Furthermore, the change in internal pressure, $\Delta p(t)$, at other frequencies can be generated by changing the actuation frequency, f_{ac}. In this study, changes in wall thickness, $\Delta h(t)$, and internal pressure, $\Delta p(t)$, were measured at multiple frequencies from 7.5 Hz to 20 Hz as shown in Fig. 6. To obtain the amplitude of the change in wall thickness, Δh_0, and that of the change in internal pressure, Δp_0, at the actuation frequency, f_{ac}, the Fourier transform was applied to those waveforms. Figures 7(a) and 7(b) show the amplitude of the change in internal pressure, Δp_0, and that of the change in wall thickness, Δh_0, respectively. The relationship between Δh_0 and Δp_0 are shown in Fig. 7(c). If the wall is purely elastic, the relationship between Δp_0 and Δh_0 always falls on the same linear line which passes through the original point. However, in Fig. 7(c), not all of the measured relationships between Δp_0 and Δh_0 fall on the same linear line. Therefore, it is found that the wall is not purely elastic.

The frequency characteristic measured using ultrasound shown in Fig. 7(c) was validated by measurement using the laser line gauge as described in §3.3. Figure 8 shows changes in internal pressure, $\Delta p(t)$, and external diameter,
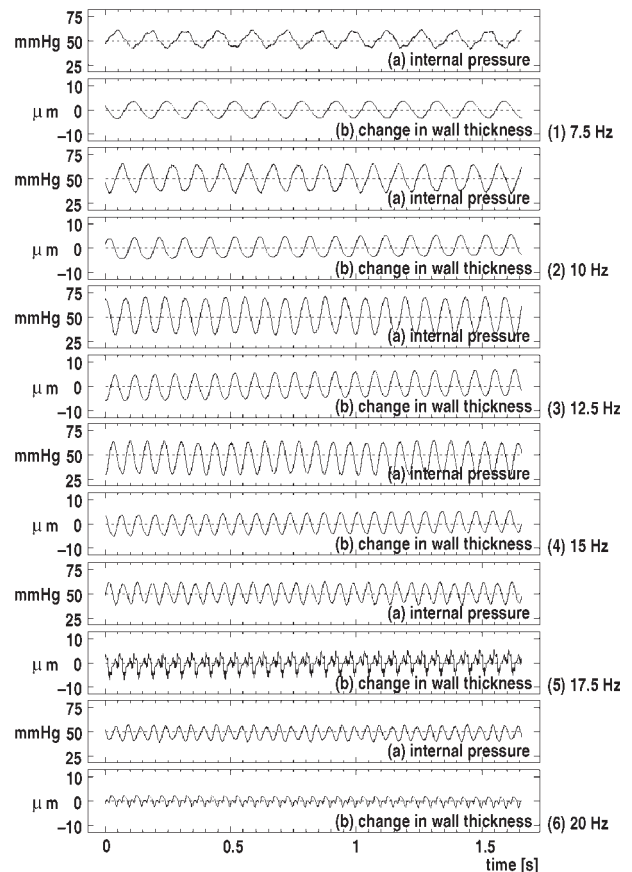

Fig. 6.   Measured changes in internal pressure, $\Delta p(t)$, and wall thickness, $\Delta h(t)$, at multiple frequencies from 7.5 Hz to 20 Hz. (a) Change in internal pressure, $\Delta p(t)$. (b) Change in wall thickness, $\Delta h(t)$.
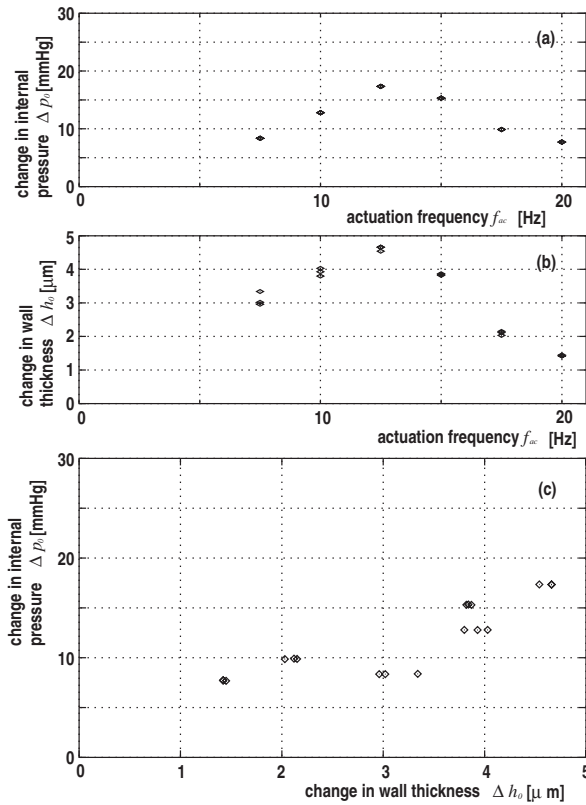
Fig. 7.　(a) Amplitude of change in internal pressure, Δp_0. (b) Amplitude of change in wall thickness, Δh_0. (c) Relationship between Δh_0 and Δp_0.

Fig. 8.　Measured changes in internal pressure, $\Delta p(t)$, and external diameter, $2\Delta r_e(t)$, at multiple frequencies from 7.5 Hz to 20 Hz. (a) Change in internal pressure, $\Delta p(t)$. (b) Change in external diameter, $2\Delta r_e(t)$.

$2\Delta r_e(t)$, at each actuation frequency, f_{ac}, from 7.5 Hz to 20 Hz. As in Fig. 7, Figs. 9(a) and 9(b) show the amplitude of the change in internal pressure, Δp_0, and that of the change in external diameter, $2\Delta r_{e0}$, respectively. In Fig. 9(c), not all of the measured relationships between Δp_0 and $2\Delta r_{e0}$ fall on the same linear line, as in the ultrasonic measurement.

From the amplitude of the change in internal pressure, Δp_0, and that of the change in wall thickness, Δh_0, as shown in Fig. 7, the elastic modulus, $|E_\theta^h|$, was obtained using eq. (2.10) at each actuation frequency, f_{ac}. The incremental elastic modulus, $|E_{inc}|$, was also obtained from the amplitude of the change in internal pressure, Δp_0, and that of the change in external diameter, $2\Delta r_{e0}$ shown in Fig. 9.

In Fig. 10, the elastic moduli, $|E_\theta^h|$, measured by the ultrasonic *phased tracking method* are shown by diamonds, which are plotted as a function of actuation frequency, f_{ac}. The elastic modulus, $|E_\theta^h|$, was measured three times at each actuation frequency with high reproducibility. In Fig. 10, it can be seen that the elastic modulus, $|E_\theta^h|$, increases with actuation frequency, f_{ac}. In Fig. 10, the elastic moduli, $|E_{inc}|$, measured using the laser line gauge are shown by squares, which are superimposed on results of the ultrasonic measurement shown by diamonds. As in the ultrasonic measurement, the elastic modulus, $|E_{inc}|$, is measured three times at each actuation frequency, f_{ac}. In Fig. 10, the elastic moduli measured using the laser line gauge have a tendency similar to those measured by ultrasound. From these results, it is found that the change in elastic modulus due to the increase in actuation frequency, f_{ac}, can be measured accurately using the ultrasonic *phased tracking method*.
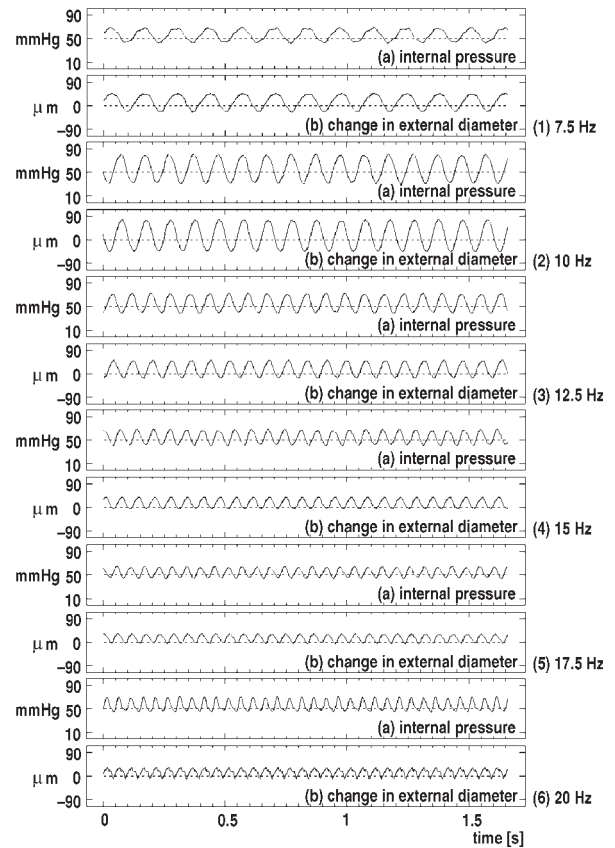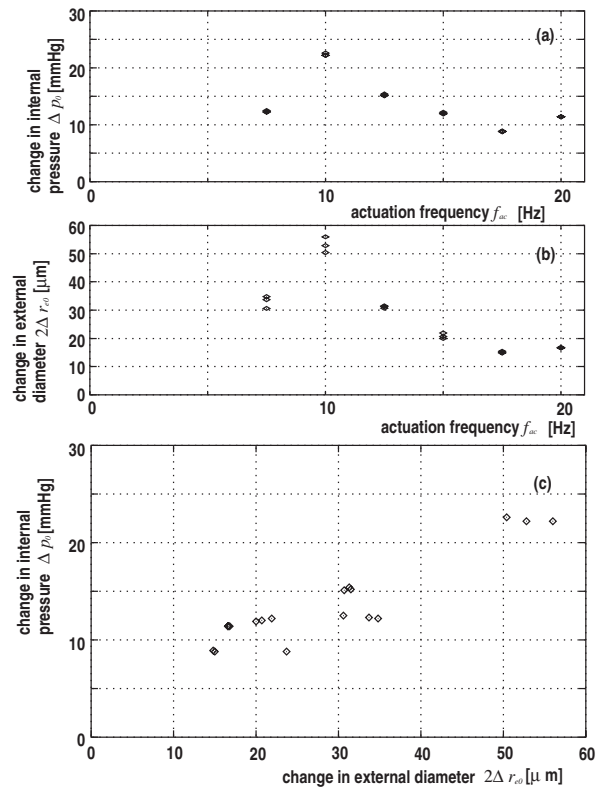

Fig. 9.　(a) Amplitude of change in internal pressure, Δp_0. (b) Amplitude of change in external diameter, $2\Delta r_{e0}$. (c) Relationship between $2\Delta r_{e0}$ and Δp_0.
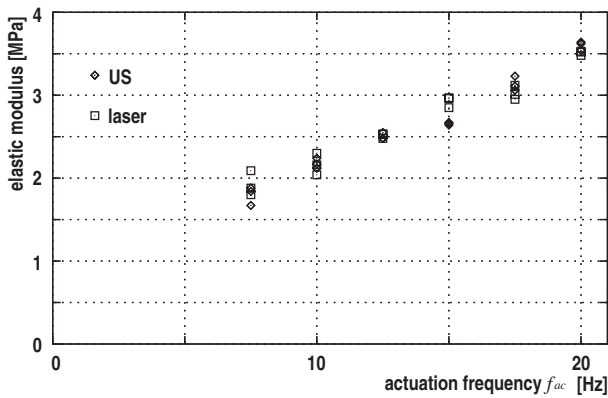
Fig. 10. Elastic moduli, $|E_\theta^h|$ and $|E_{inc}|$, at each actuation frequency, f_{ac}. Diamonds and squares show results obtained using ultrasound and those obtained using the laser line gauge, respectively.
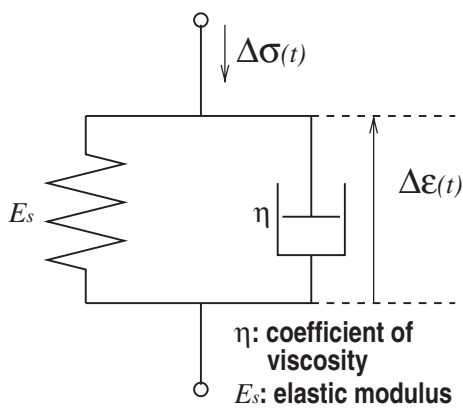

Fig. 11. Voigt model.

5. Discussion

In Fig. 10, the elastic modulus, $|E_\theta^h|$, is observed to increase with actuation frequency, f_{ac}. The reason for this is as follows: When we assume the Voigt model, which is illustrated in Fig. 11, as a viscoelastic model of the silicone rubber, the relationship between stress, $\Delta\sigma(t)$, and strain, $\Delta\varepsilon(t)$, is expressed as

$$\Delta\sigma(t) = E_s \cdot \Delta\varepsilon(t) + \eta \cdot \frac{d}{dt}\Delta\varepsilon(t), \quad (5.1)$$

where E_s and η are the static elastic modulus and the viscosity constant, respectively, and E_s and η are assumed not to be dependent on the actuation frequency, f_{ac}. In eq. (5.1), $\Delta\varepsilon(t)$ and $\Delta\sigma(t)$ correspond to $-\Delta\varepsilon_r(t) = -\Delta h(t)/h_0$ and $(r_0/h_0 + 1)\Delta p(t)/2$ in eq. (2.9), respectively.

By defining $\Delta\sigma(t) = \Delta\sigma_0 \cdot e^{j2\pi f_{ac}t}$ and $\Delta\varepsilon(t) = \Delta\varepsilon_0 \cdot e^{j(2\pi f_{ac}t - \theta)}$, eq. (5.1) can be rewritten as

$$\Delta\sigma(t) = E_s \cdot \Delta\varepsilon(t) + j2\pi f_{ac}\eta \cdot \Delta\varepsilon(t), \quad (5.2)$$

where $\Delta\sigma_0$ and $\Delta\varepsilon_0$ are the amplitude of the stress and that of the strain, respectively.

From eq. (5.2), the complex elastic modulus, $E_{Voigt} = \Delta\sigma(t)/\Delta\varepsilon(t)$, is expressed as

$$E_{Voigt} = \frac{\Delta\sigma(t)}{\Delta\varepsilon(t)}$$

$$= E_s + j2\pi f_{ac}\eta$$

$$= \sqrt{E_s^2 + (2\pi f_{ac}\eta)^2} \cdot e^{j\theta}, \quad (5.3)$$

$$\theta = \tan^{-1}\left(\frac{2\pi f_{ac}\eta}{E_s}\right). \quad (5.4)$$

In eq. (5.3), it is found that the absolute value of the complex elastic modulus of the Voigt model increases with the frequency of the applied stress, and such frequency characteristics can be observed in the elastic modulus measured using ultrasound, as shown by diamonds in Fig. 10.

From these results, it is found that the measurement of elastic moduli, $|E_\theta^h|$, at multiple frequencies is useful in the assessment of viscoelastic property. To determine the frequency characteristic of elastic modulus, $|E_\theta^h|$, it is necessary to induce changes in internal pressure at multiple frequencies. This study yielded significant results demonstrating that changes in internal pressure at multiple frequencies can be induced by remotely applied actuation and that the resultant minute change in wall thickness can be measured by our *phased tracking method*.

Let us consider the application of the proposed method to actual *in vivo* measurements. Under *in vivo* conditions, the deformation of the arterial wall caused by remote actuation will be influenced by tissues surrounding the artery. When the proposed method is applied to the artery deep inside the body, the influence of the surrounding tissues will be significant. Therefore, we intend to apply the proposed method to a superficial artery, *i.e.* the carotid artery. Since the carotid artery is mainly surrounded by a thin subcutaneous layer of fats and muscles, the influence of the surrounding tissues is supposed to be not significant because the artery is covered and restricted by the adventitia (mainly composed of collagen fiber) which is harder than the surrounding tissues. Furthermore, using the method previously proposed by our group,[23,25] the elastic modulus of a femoral artery was measured in an *in vivo* experiment before surgery and an *in vitro* experiment using a water tank and an artificial heart after the surgical extraction. The difference between the average elastic modulus before and that after extraction was about 8% (0.96 ± 0.48 MPa: before extraction, 0.89 ± 0.31 MPa: after extraction). Thus, the influence of the surrounding tissues can be neglected in the cases of superficial arteries.

In actual *in vivo* measurement at the carotid artery, one way of generating a cyclic change in blood pressure is to apply actuation on the skin surface above the brachial artery and measure the change in wall thickness due to remote actuation at the carotid artery.

To realize the proposed method in the *in vivo* measurement, a method of measuring the change in blood pressure caused by remote actuation must be established. It is reported that the waveform of the change in artery diameter almost corresponds to that of the change in blood pressure due to the heartbeat.[27] Therefore, the change in blood pressure is supposed to be estimated using the waveform of the change in artery diameter with blood pressure by calibration using the systolic and diastolic pressures. However, if the same changes in blood pressure are caused by

remote actuation at different frequencies, changes in artery diameter will be different due to the viscoelasticity of the arterial wall. Thus, it is difficult to calibrate the change in diameter. An alternative way of measuring blood pressure is to use applanation tonometry,[28] which measures the continuous waveform of blood pressure by applanation of the radial artery using a pressure detector for measuring the stress caused by the change in blood pressure.

Since the stress-strain relationship of the arterial wall is nonlinear, the elastic property of the arterial wall changes during one cardiac cycle due to the change in blood pressure caused by the heartbeat. Therefore, in *in vivo* measurement, the amplitude of the change in wall thickness and that of the change in blood pressure must be estimated during each short period by applying short-time Fourier transform. However, it is difficult to measure elastic modulus at different frequencies during one cardiac cycle because the actuation frequency cannot be changed during such a short period. This problem can be overcome by changing actuation frequency per heartbeat. By referring to the electrocardiogram, elastic modulus at different frequencies can be measured at the same time (= similar blood pressure) during the cardiac cycle.

As mentioned above, although there are many things to consider in order to realize the proposed method in an actual *in vivo* measurement, the most important problem to overcome is the measurement of the change in blood pressure due to remote actuation. Further investigation is necessary to measure blood pressure under *in vivo* conditions.

6. Conclusions

In this study, basic experiments were performed to assess the viscoelastic properties of the arterial wall. If the wall is viscoelastic, elastic modulus changes with the frequency of the applied stress. To investigate the frequency characteristic of elastic modulus, it is necessary to generate changes in internal pressure at multiple frequencies. In this study, the results of basic experiments using a silicone rubber tube demonstrated that changes in internal pressure at multiple frequencies can be generated by remotely applied actuation. By measuring the resultant minute change in wall thickness by our *phased tracking method*, the frequency characteristic of elastic modulus is obtained. These results suggest that remote actuation has potential for application to the assessment of viscoelastic properties due to its ability to change the frequency of the stress.

1) S. Glagov, E. Weisenberg, C. K. Zarins, R. Stankunavicius and G. J. Kolettis: New Engl. J. Med. **316** (1987) 1371.
2) R. T. Lee, A. J. Grodzinsky, E. H. Frank, Roger D. Kamm and F. J. Schoen: Circulation **83** (1991) 1764.
3) H. M. Loree, A. J. Grodzinsky, S. Y. Park, L. J. Gibson and R. T. Lee: J. Biomech. **27** (1994) 195.
4) P. C. G. Simons, A. Algra, M. L. Bots, D. E. Grobbee and Y. van der Graaf: Circulation **100** (1999) 951.
5) E. Falk, P. K. Shah and V. Fuster: Circulation **92** (1995) 657.
6) M. J. Davies: Circulation **94** (1996) 2013.
7) J. Golledge, R. M. Greenhalgh and A. H. Davies: Stroke **31** (2000) 774.
8) A. P. G. Hoeks, C. J. Ruissen, P. Hick and R. S. Reneman: Ultrasound Med. Biol. **11** (1985) 51.
9) T. Länne, H. Stale, H. Bengtsson, D. Gustafsson, D. Bergqvist, B. Sonesson, H. Lecerof and P. Dahl: Ultrasound Med. Biol. **18** (1992) 451.
10) A. P. G. Hoeks, X. Di, P. J. Brands and R. S. Reneman: Ultrasound Med. Biol. **19** (1993) 727.
11) P. J. Brands, A. P. Hoeks, M. C. Rutten and R. S. Reneman: Ultrasound Med. Biol. **22** (1996) 895.
12) J. M. Meinders, P. J. Brands, J. M. Willigers, L. Kornet and A. P. G. Hoeks: Ultrasound Med. Biol. **27** (2001) 785.
13) D. H. Bergel: J. Physiol. **156** (1961) 445.
14) L. H. Peterson, R. E. Jensen and J. Parnell: Circ. Res. **8** (1960) 622.
15) K. Hayashi, H. Handa, S. Nagasawa, A. Okumura and K. Moritake: J. Biomech. **13** (1980) 175.
16) H. Kanai, M. Sato, Y. Koiwa and N. Chubachi: IEEE Trans. Ultrason., Ferroelect., Freq. Control **43** (1996) 791.
17) H. Kanai, H. Hasegawa, N. Chubachi, Y. Koiwa and M. Tanaka: IEEE Trans. Ultrason., Ferroelect., Freq. Control **44** (1997) 752.
18) H. Hasegawa, H. Kanai, N. Chubachi and Y. Koiwa: Electron. Lett. **33** (1997) 340.
19) H. Hasegawa, H. Kanai, N. Chubachi and Y. Koiwa: Jpn. J. Med. Ultrason. **24** (1997) 851.
20) H. Hasegawa, H. Kanai, N. Hoshimiya, N. Chubachi and Y. Koiwa: Jpn. J. Appl. Phys. **37** (1998) 3101.
21) H. Kanai, K. Sugimura, Y. Koiwa and Y. Tsukahara: Electron. Lett. **35** (1999) 949.
22) H. Hasegawa, H. Kanai, N. Hoshimiya and Y. Koiwa: Jpn. J. Appl. Phys. **39** (2000) 3257.
23) H. Hasegawa, H. Kanai, N. Hoshimiya and Y. Koiwa: Jpn. J. Med. Ultrason. **28** (2001) 3.
24) H. Hasegawa, H. Kanai and Y. Koiwa: Jpn. J. Appl. Phys. **41** (2002) 3563.
25) H. Hasegawa, H. Kanai, Y. Koiwa, M. Ichiki and F. Tezuka: to be published in *IEEE 2002 Int. Ultrason. Symp. Proc.* (2002).
26) A. G. Hudetz: J. Biomech. **12** (1979) 651.
27) M. Sugawara, H. Furuhata, S. Kikkawa, S. Suzuki, S. Ohnishi, W. Takabayashi, N. Suzuki, T. Kurokawa, S. Yoshimura and C. G. Caro: Jpn. J. Med. Electron. Biol. Eng. **21** (1983) Suppl. 429.
28) J. D. Cameron, B. P. Mcgrath and A. M. Dart: J. Am. Coll. Cardiol. **32** (1998) 1214.